International Journal of Agriculture and Biosciences 2026 15(1): 225-232.
https://doi.org/10.47278/journal.ijab/2025.156

RESEARCH ARTICLE
eISSN: 2306-3599; pISSN: 2305-6622

Green Nanomaterial of Clammy inula (*Inula viscosa* L.) as an Effectual Antifungal for *Fusarium oxysporum*

Wisam M. Obeidat [1,*], Kholoud M. Alananbeh [1], Nour S. AbuShanab [1], Afnan Al-Hunaiti [2] and Sharif Arar [2]

[1]The University of Jordan, School of Agriculture, Department of Plant Protection, Amman 11942, Jordan
[2]The University of Jordan, School of Science, Department of Chemistry, Amman 11942, Jordan
*Corresponding author: wi.obeidat@ju.edu.jo

ABSTRACT

Clammy inula (*Inula viscosa* L.) is a native Meditranean perennial herb/shrub. It's antifungal activity against different plant pathogens has been proven by several studies; however, none of these studies investigated the antifungal activity of green nanomaterials extracted from *I. viscosa* against controlling plant pathogens. This research investigated the antifungal activity of green nanomaterials, specifically nickel and zinc nanoferrites derived from *I. viscosa* (interactions), against controlling *F. oxysporum*. The aim was to evaluate the efficacy of nanomaterials derived from both leaves and pappus of *I. viscosa*, and to assess the synergistic effects of combining these nanomaterials with *I. viscosa* extracts against *F. oxysporum*. Treatments, nanomaterials, and their interactions significantly influenced fungal growth rate and colony inhibition. The lowest average fungal growth rate (34.1%) was observed with the combination of *I. viscosa* leaves extract and $NiFe_2O_4$ nanomaterials, while the highest growth rate (68.5%) was recorded with leaf extract alone. The highest average inhibition rate of fungal colony growth (50.2%) was also observed with the interaction between leaves extract and $NiFe_2O_4$. The results were supported by UV spectra that confirmed the occurrence of nanoferrites. Clammy inula contains active bioingredients that are considered superior molecules for cell penetration. These findings suggest that the combination of plant leaf extract and green nanomaterials exhibits a synergistic antifungal effect against *F. oxysporum*.

Keywords: Nanoferrites; Nanomaterials, UV-Visible; Synthesis.

Article History
Article # 25-411
Received: 16-Jul-25
Revised: 03-Aug-25
Accepted: 13-Aug-25
Online First: 21-Sep-25

INTRODUCTION

Inula viscosa syn. (*Dittrichia viscosa*), is a widespread perennial weed species native to the Mediterranean region. *I. viscosa* plants belong to the Asteraceae family. Plant extraction from leaves and stems has been assayed for different biological activities as antimicrobials (Vuko et al., 2021), allelopathy, controlling the growth and development of insects, nematodes, and has antifungal activities in invitro and in the field (Grauso et al., 2020; Boari et al., 2021). Botanical fungicides could be a good alternative to chemical control of most fungal diseases in the Integrated Pest Management (IPM). *I. viscosa* water extract was proved to have antifungal effects against *Pseudoperonospora cubensis*, *Phytophthora infestanson*, and *Puccinia helianthin* (Pane et al., 2023). Methanol extraction proved its antifungal effect against *Alternaria solani, Rhizoctonia solani* and *Fusarium oxysorum* f.sp *melonis* (Abou-Jawdah et al., 2004).

Several species of *I. viscosa* have been used for their antifungal properties against plant pathogens, including *Fusarium culmorum* and *F. graminearum* (Haoui et al., 2015). The *Fusarium* genus comprises a diverse group of species that are widely distributed as soil-borne fungi, which are associated with plant diseases (Chehri, 2011). *F. oxysporum* has a wide host range, causing significant economic losses in major crops such as tomatoes, soybeans, cucumbers, and melons (Snyder & Hansen, 1940). This pathogen is responsible for vascular wilt diseases, affecting both plant shoots and roots, leading to substantial yield reductions (Edel-Hermann & Lecomte, 2019). Belabid et al. (2010) reported that the powders of *I. viscosa* significantly reduce the soil population densities of *Fusarium oxysporum* f. sp. *lentis* Vasudeva and Srinivasan (Fol) and the disease incidence on lentil.

Cite this Article as: Obeidat WM, Alananbeh KM, AbuShanab NS, Al-Hunaiti A and Arar S, 2026. Green nanomaterial of Clammy inula (*Inula viscosa* L.) as an effectual antifungal for *Fusarium oxysporum*. International Journal of Agriculture and Biosciences 15(1): 225-232. https://doi.org/10.47278/journal.ijab/2025.156

A Publication of Unique Scientific Publishers

The extensive use of fungicides in recent years has led to a growing concern over fungicide resistance, posing a major challenge in fungal disease management. The effectiveness of available fungicides is declining, necessitating alternative control strategies. The synthesis and application of nanomaterials offer a promising approach to enhance the efficacy of plant-derived antifungal compounds by improving their penetration, solubility, and bioavailability, while also extending their activity duration (Zargar et al., 2023).

Recently, in the agricultural sector, nanoparticle products have shown promising results, including management of several pathogens such as *Xanthomonas*, *Aspergillus* spp., *Botrytis cinerea*, and *Fusarium* spp. (Alghuthaymi et al., 2021). For example, *Brassica juncea, Medicago sativa*, and *Sesbania* plant species are used to synthesize green nanoparticles (Shang et al., 2019). None of these studies investigated the antifungal activity of green nanomaterials extracted from *I. viscosa* against controlling plant pathogens. Therefore, this study aimed to investigate the antifungal activity of green nanomaterials derived from *I. viscosa* against controlling *F. oxysporum*. The study objective is to evaluate the antifungal activity of green nanomaterials derived from *I. viscosa* against *F. oxysporum*. By (1) assessing the antifungal potential of green nanomaterials extracted solely from *I. viscosa*, (2) comparing the antifungal efficacy of nanomaterials synthesized *I. viscosa* pappus with those derived from its leaves, and (3) exploring the potential synergistic antifungal effect of combining synthesized green nanomaterials with extracts from *I. viscosa* (either leaves or pappus) against *F. oxysporum*.

MATERIALS & METHODS

Clammy Inula Source and Extraction

In October, one kilogram of *I. viscosa* leaves and pappus were collected at the flowering stage from Jubiha (32°1′23.394″N; 35°53′30.973″E), Jordan. The collected specimens were transferred to the University of Jordan. *I. viscosa* leaves and pappus were dried at room temperature for four weeks and stored in paper bags at room temperature until further use.

For plant extraction, harvested *I. viscosa* materials, including leaves (L) and pappus (P) were ground into fine powder. A total of 200g of the dried ground material (either L or P) was extracted at 35°C by shaking for 24h in a solvent mixture of acetone and *n*-hexane (9:1, v/v) at a ratio of 1:10 (w/v, dry plant material/solvent). This extraction procedure targets fractions that are slightly polar organic molecules, including sesquiterpene lactones, tomentosin, and iso-costic acid, with slight solubility in water reported previously by Shtacher & Kashman (1970). The extract was then filtered using Whatman No.1 filter paper and dried in an oven at 40°C to obtain dry pappus and a green paste. Two grams from each extract (either dry green paste or dry pappus) were dissolved in 100mL of acetone. The solution was heated on a hot plate at 40°C for 15min while continuously mixed using a magnetic stirrer. The extract was then filtered through Whatman No.1 filter paper and diluted to prepare a series of concentrations (2, 1, 0.5, and 0.25% w/v) using acetone as a solvent.

Synthesis of Green Nanoparticles

To prepare the nanomaterials, *I. viscosa* plant extract was thoroughly washed several times. A total of 200g of plant segments was ground and mixed with 200mL of distilled water, followed by refluxing at 90˚C for 3 hours. The resulting extract was filtered and subsequently used for nanoparticle synthesis. The synthesis of the $NiFe_2O_4$ nanoparticles was carried out following the method described by Al-Hunaiti et al. (2021), while the $ZnFe_2O_4$ nanoparticles were synthesized according to Al-Hunaiti et al., (2020), using *I. viscosa* extract as a reducing and stabilizing agent. Where briefly in the preparation steps the solutions were stirred at room temperature until they were homogenized. Then, 50mL of the plant extract was added dropwise to the solutions with continuous stirring for 30 minutes. After a few steps, the mixture was then sonicated (Ultrasonic Cleaner, Fisher Scientific, USA) for 15 minutes and dried in an oven (Memmert, Germany) at 80°C overnight. After being repeatedly cleaned with distilled water, the resulting dry powder was allowed to dry in the oven for two hours, and then left to cool in a desiccator. The green extract of *I. viscosa* green nanoparticles were stacked in zipper bags and kept at -20°C for long storage periods, while some portions were kept in the refrigerator at 5°C for daily use. The green extract nanoparticles could stand and be stable on lab shelves up to six months or more. For daily use as quoted from Qin et al. (2021), "Spinel material, as an effective noble-metal-free alternative, is recognized as a low-cost non-precious electrocatalyst taking advantages of their high element abundance, low cost, environmental friendliness, and high performance. Studies have proved that mixed metal oxide compounds are potential candidates for electrocatalytic reactions. As bimetallic oxides, spinel ferrites have received great attention in the electrocatalysis field." The Two grams of each nanomaterial (either $NiFe_2O_4$ or $ZnFe_2O_4$) was added to 100mL of acetone. The solution was heated on a hot plate at 40°C for 15min while being continuously stirred using a magnetic stirrer. The nanomaterials were then filtered using Whatman No.1 filter paper and diluted to prepare a series of concentrations (2, 1, 0.5, and 0.25% w/v) using acetone as the solvent.

For the preparation of nanoparticle-extract interactions, plant extracts (either L or P) were mixed with nanoparticles (either $NiFe_2O_4$ or $ZnFe_2O_4$) in a 1:1 ratio to obtain the final product.

Antifungal Activity of Synthesized NPs against *F. oxysporum* in vitro

A 6mm diameter mycelial disc from a 10-days-old culture of *F. oxysporum* was placed near the periphery of the PDA plate. The isolate was previously isolated from banana roots (Kholoud M. Alananbeh, unpublished). On the opposite side of the plate, a 6mm agar disc was aseptically removed, and 100µL of the nanomaterial or plant extract treatment was applied in its place using a 10–100µL mechanical micropipette (Ratiopetta®). The inoculated

plates were incubated in a growth chamber at 27±1°C. Each treatment was tested with three replicates.

For mycelium growth rate (MGR), colony growth was recorded after 3, 8, and 13 days. For each treatment, the average of two perpendicular colony diameter measurements was recorded and analyzed using the following equation:

MGR%=(The average diameter of mycelial growth in treatment (mm)/number of days) × 100%

To assess the antifungal activity, the diameter of the inhibition zone surrounding each well was measured. The mean inhibition of colony growth for each treatment was calculated using the following equation:

ICGR%=(1- The average diameter of mycelial growth in treatment (mm)/ The average diameter of mycelial growth in control (mm)) × 100%

UV-Visible Characterization

Leaves (L), Pappus (P) extracts (indicated in this work as treatment), and interaction samples (green nanoparticles) were subjected to UV-visible analysis in the range 200 - 800nm using UV-Vis, Varian Cary 100 bio, Dual Beam spectrophotometer. Measurements were done using analytical grade acetone as a blank. This was done to observe the maximum absorption regions (λ_{max}), absorbance values for the presence and occurrence of the active constituents of *Inula viscosa* L extracts in acetone, as previously reported (tomentose, inuviscolide, Costic acid and iso-costic acid, and other possible polyphenols and flavonoids) (Shtacher & Kashman 1970; Mamoci et al., 2011; Rechek et al., 2023) Also detecting any UV-spectrum changes for the active constituents in the presence of the nano-particles $NiFe_2O_4$ or $ZnFe_2O_4$ that could indicate the occurrence of any metal-chelates or complexes/ adducts (Bouttier-Figueroa et al., 2023).

Statistical Analysis

Statistical analyses were performed using the PROC GLIMMIX procedure of SAS 9.4. Data were analyzed using analysis of variance (ANOVA). To evaluate the factors influencing fungal growth rate (%) and inhibition of colony growth rate (%). The experiment was designed as a Complete randomized design (CRD) with three factors: plant extraction (leaves or pappus), nanomaterials ($NiFe_2O_4$ or $ZnFe_2O_4$), and concentration (2, 1, 0.5, and 0.25% w/v). The Shapiro-Wilk statistic of PROC UNIVARIATE in SAS was used to test for normality of the distribution of errors and ensure the mean of residuals equaled to zero. The experiment was replicated three times. The replications were considered as random effects. The treatments, nanomaterials, and concentration were considered as fixed effects. The F- test was used to test significant sources of variance of the model. The total variance was partitioned into different effects replication, treatment, nanomaterial, and treatment × nanomaterial interaction.

Then, each parameter was analyzed at different concentrations. The total variance was partitioned into different effects: replication, treatment, nanomaterial, concentration, treatment × nanomaterial, and treatment × nanomaterial × concentration. Post-hoc multiple comparisons were performed using Tukey's Honest Significant Difference (HSD) test at a significance level of P=0.05 for all analyses.

RESULTS

Percent Growth Rate (PGR)

The results demonstrate significant differences in fungal growth inhibition across different treatments, nanomaterials, and their interactions over time (3, 8, and 13 days) (Table 1, Fig. 1). At all-time points, the untreated *F. oxysporum* control exhibited the highest fungal growth rates, confirming its aggressive nature in the absence of antifungal agents. Similarly, $ZnFe_2O_4$ nanoparticles alone did not significantly reduce fungal growth compared to the untreated control, suggesting a weaker antifungal effect when applied alone.

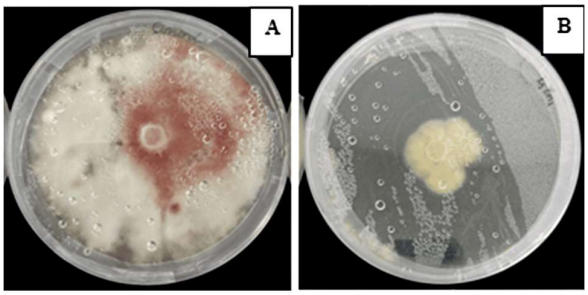

Fig. 1: *F. oxysporum* colony after thirteen days of incubation at 27°C on potato dextrose agar (PDA): a) Control; and b) L×$ZnFe_2O_4$(2%).

Table 1: The mean percentage of fungal growth rate of *F. oxysporum* after 3 days, 8 days, and 13 days. *P-value* analysis of variance to determine the importance of treatments, nanomaterials, and concentrations, and their interaction affecting the percentage of fungal growth rate

Time Parameter		3 days	8 days	13 days
		.....Mean[2].....		
Treatment	Leaves (L)	81.1[a]	84.5[a]	68.5[a]
	Pappus (P)	76.0[ab]	81.8[a]	67.3[a]
	Acetone	59.4[bc]	70.2[ab]	67.8[ab]
	F. oxysporum	91.7[a]	91.3[a]	68.2[ab]
NPs[1]	$NiFe_2O_4$	51.8[c]	54.4[bc]	52.1[b]
	$ZnFe_2O_4$	85.0[a]	83.3[a]	67.4[a]
Interaction	L×$NiFe_2O_4$	36.8[d]	31.1[d]	34.1[c]
	L×$ZnFe_2O_4$	35.6[d]	38.4[cd]	34.9[c]
	P×$NiFe_2O_4$	36.9[d]	32.0[d]	36.7[c]
	P× $ZnFe_2O_4$	37.5[d]	35.0[d]	37.0[c]
ANOVA		3 days	8 days	13 days
Source		DF	*P*-value	
Treatments (T)		3 0.0005	0.0002	0.1984
Concentration (C)		3 0.344	0.472	0.779
Nanomaterials (N)		1 <.0001	<.0001	<.0001
T×N		3 0.958	0.011	0.026

1NPs.= Nanomaterials; 2Columns values with different letters significantly different at alpha=0.05 according to Tukey last significant differences test

In contrast, treatments incorporating $NiFe_2O_4$ nanoparticles, either alone or in combination with plant extracts, resulted in substantial fungal growth suppression. Among these, the interaction of $NiFe_2O_4$ with plant extracts (L × $NiFe_2O_4$ and P × $NiFe_2O_4$) showed the greatest inhibition, with fungal growth rates significantly lower than other treatments. This suggests a synergistic antifungal effect between the plant extracts and the $NiFe_2O_4$ nanoparticles. The lowest growth rate recorded was in the P × $NiFe_2O_4$ interaction (36.9% at 3 days, 32.0% at 8 days, and 36.7% at 13 days), highlighting its potential as an effective antifungal treatment (Table 1).

Statistical analysis (ANOVA) confirms the significant effect of treatments (P<0.0001) and nanomaterials (P<0.0001) on fungal growth across all time points. However, the concentration factor was not statistically significant (P>0.344), indicating that the tested concentrations of treatments did not drastically alter the overall trend of inhibition. The interaction between treatments and nanomaterials was significant (0.011 and 0.026 for 8 and 13 days, respectively), further supporting the combined effect of plant extracts and nanomaterials in reducing *F. oxysporum* growth (Table 1).

Percent Inhibition of Colony Growth Rate (PICGR)

The PICGR after three days was significant. The results indicate significant differences in the inhibition of *F. oxysporum* colony growth across different treatments, nanomaterials, and their interactions over time (3, 8, and 13 days) (Table 2). At 3rd day, the highest inhibition rates were observed in treatments that combined $NiFe_2O_4$ or $ZnFe_2O_4$ nanoparticles with plant extracts, with P × $NiFe_2O_4$ (59.8%) and P × $ZnFe_2O_4$ (59.2%) exhibiting the most potent effects. In contrast, the lowest inhibition rates were observed in the treatments containing $ZnFe_2O_4$ alone (7.6%) and leaves extract alone (11.8%), indicating that $ZnFe_2O_4$ alone had weak antifungal activity. The control treatment with acetone (35.4%) also showed moderate inhibition (Table 2).

Table 2: The mean percent inhibition of colony growth rate of *F. oxysporum* after 3 days, 8 days, and 13 days. *P-value* of analysis of variance to determine the importance of treatments, nanomaterials, concentrations, and their interaction affecting the percentage of fungal inhibition

Time Parameter		3 days		8 days	13 days
				Mean[2]	
Treatment	Leaves (L)	11.8^{d}		7.2^{cd}	0^{d}
	Pappus (P)	17.4^{cd}		10.1^{cd}	1.7^{d}
	Aceton	35.4^{bc}		22.9^{c}	0.9^{d}
NPs[1]	$NiFe_2O_4$	43.7^{b}		40.3^{b}	23.9^{c}
	$ZnFe_2O_4$	7.6^{d}		8.4^{cd}	1.5^{d}
Interaction	L×$NiFe_2O_4$	59.9^{a}		65.8^{a}	50.2^{ab}
	L×$ZnFe_2O_4$	61.4^{a}		74.6^{a}	49.1^{a}
	P×$NiFe_2O_4$	59.8^{a}		64.9^{a}	46.4^{b}
	P× $ZnFe_2O_4$	59.2^{a}		61.6^{a}	45.9^{b}
ANOVA		3 days		8 days	13 days
Source		DF		*P*-value	
Treatments (T)		1	0.007	0.01	0.801
Concentration (C)		3	0.08	0.136	0.111
Nanomaterials (N)		1	<.0001	<.0001	0.0022
T×N		7	0.958	0.011	0.026
T×N×C		15	<.0001	<.0001	0.0007

1NPs.= Nanomaterials; 2Columns values with different letters are significantly different at alpha=0.05 according to Tukey last significant differences test.

At 8 days, a similar trend was observed, with the combined treatments of $NiFe_2O_4$ and $ZnFe_2O_4$ nanoparticles with plant extracts (P × $NiFe_2O_4$, P × $ZnFe_2O_4$, L × $NiFe_2O_4$, L × $ZnFe_2O_4$) continuing to show the highest inhibition rates (ranging from 61.6% to 74.6%). Meanwhile, treatments containing plant extracts alone (L: 7.2%, P: 10.1%) and $ZnFe_2O_4$ alone (8.4%) remained less effective (Table 2). At 13 days, the inhibition was still noticed to be highest in the interaction treatments (above 45%), confirming a synergistic antifungal effect between plant extracts and nanoparticles. The inhibition from nanoparticles alone ($NiFe_2O_4$: 23.9%, $ZnFe_2O_4$: 1.5%) and plant extracts alone (L: 0%, P: 1.7%) had significantly decreased, indicating that nanoparticles alone provided low ($ZnFe_2O_4$) to moderate ($NiFe_2O_4$) inhibition; their combination with plant extracts had a more prolonged antifungal effect (Table 2).

The ANOVA results showed that the effects of treatments (T) were highly significant at 3 days (P=0.007) and 8 days (P=0.01), but not at 13 days (P=0.801), indicating that the effectiveness of treatments diminished over time. The impact of nanomaterials (N) remained significant throughout all time points (P<0.0001 to P=0.0022), confirming their strong role in fungal inhibition. Additionally, the interaction between treatments and nanomaterials (T × N) was significant across 8 and 13 days (P=0.011 and 0.026, respectively), further reinforcing the enhanced antifungal activity observed when nanoparticles were combined with plant extracts (Table 2).

Treatment × nanoparticles × concentration (T × N × C), the interaction between T × N × C was highly significant across all time points, indicating that plant dry parts perform differently in different nanoparticle concentrations (Table 2). At the beginning the highest fungal percentage inhibition of radial mycelia growth rate after three days was obtained from L × $NiFe_2O_4$ (2%) (64%), P × $NiFe_2O_4$ (0.5%) (64%), P × $ZnFe_2O_4$ (0.5%) (63%), and L × $ZnFe_2O_4$ (2%) (63%) (Table 3). However, the lowest fungal percentage inhibition of radial mycelia growth rate was obtained from L × $ZnFe_2O_4$ (0.25%) (17%) (Table 3). After eight days, the highest percentage inhibition of *F. oxysporum* mycelia growth rate was observed in L × $ZnFe_2O_4$ (2%) (77%), L × $ZnFe_2O_4$ (0.5%) (74%), L × $ZnFe_2O_4$ (1%) (73%), and L ×$NiFe_2O_4$ (1%) (70%). The lowest *F. oxysporum* percent inhibition of radial mycelia growth rate was observed in L × $ZnFe_2O_4$ (0.25%) (7%). At the end of the experiment (13 days) the highest *F. oxysporum* percent inhibition of radial mycelia growth rate were observed in L × $ZnFe_2O_4$ (2%) (71%), L × $ZnFe_2O_4$ (1%) (66%), L × $ZnFe_2O_4$ (0.5%) (59%), and P × $NiFe_2O_4$ (0.25%) (58%), while the lowest percentage inhibition of *F. oxysporum* mycelia growth rate was observed in L × $ZnFe_2O_4$ (0.25%) (0.1%) (Table 3).

Table 3: The mean percent inhibition of colony growth rate of *F. oxysporum* after 3 days, 8 days and 13 days and the absorbance values for interaction samples at 330 and 356nm

Time and UV T×N×C	3 days	8 days	13 days	UV absorption at 330±4 nm	UV absorption at 356±4 nm
	Mean[1]				
P×$NiFe_2O_4$ (0.25%)	57^{a}	64^{ab}	58^{a}	0.13	0.00
P×$NiFe_2O_4$ (0.5%)	64^{a}	63^{ab}	29^{ab}	0.21	0.00
P×$NiFe_2O_4$ (1%)	60^{a}	65^{ab}	44^{ab}	0.60	0.40
P×$NiFe_2O_4$ (2%)	58^{a}	68^{ab}	54^{a}	1.46	0.93
P×$ZnFe_2O_4$ (0.25%)	51^{a}	49^{b}	35^{ab}	0.12	0.00
P×$ZnFe_2O_4$ (0.5%)	63^{a}	65^{ab}	48^{a}	0.55	0.00
P×$ZnFe_2O_4$ (1%)	61^{a}	66^{a}	50^{a}	1.29	0.90
P×$ZnFe_2O_4$ (2%)	61^{a}	66^{ab}	51^{a}	1.49	0.94
L×$NiFe_2O_4$ (0.25%)	55^{a}	61^{ab}	54^{a}	0.1	0.00
L×$NiFe_2O_4$ (0.5%)	53^{a}	62^{ab}	48^{a}	0.14	0.00
L×$NiFe_2O_4$ (1%)	56^{a}	70^{ab}	56^{ab}	0.53	0.00
L×$NiFe_2O_4$(2%)	64^{a}	65^{ab}	39^{ab}	2.40	1.53
L×$ZnFe_2O_4$ (0.25%)	17^{b}	7^{c}	0.1^{b}	0.15	0.00
L×$ZnFe_2O_4$ (0.5%)	61^{a}	74^{ab}	59^{a}	0.65	0.00
L×$ZnFe_2O_4$ (1%)	61^{a}	73^{ab}	66^{a}	0.90	0.57
L×$ZnFe_2O_4$(2%)	63^{a}	77^{a}	71^{a}	2.16	1.30

1Columns values with different letters are significantly different at alpha=0.05 according to Tukey last significant differences test.

UV-Visible Scanning Results

The UV-visible spectrum of the treatment and interaction samples indicated the presence of three absorption maxima at 207±2, 330±4, and 356±4nm, as demonstrated for some samples in Fig. S1-S8. The UV spectrum of the interaction versus treated showed nearly no red or blue shifts, but a significant reduction in absorbance intensities at the two wavelengths 330nm (mainly) and 356nm for most of the samples as summarized in Table 3 and Table 4. The reduction in UV absorbance values is due to the reduction and chelation action of the active constituents of *I. viscosa* (tomentosin, inuviscolide, costic acid and iso-costic acid, and other possible polyphenols and flavonoids) to the metals Zn and Ni to produce metal and metal oxide nanoparticles associated with oxidized forms of the active constituents (polyphenol, flavonoid) for the substituted hydroxy groups into may be carbonyls, quinones, and keto groups with intermediated metal-ligands structures that could affect total aromaticity and conjugation of the original secondary metabolites structures leading to reduced mainly ππ* transitions and ultimately reducing molar absorptivity (€) according to Beers law (A= €bC) where b is the optical pathlength in cm and C is the concentration in molarity, ending up with reduced absorbance for the green extract nano particles (interactions) as reported previously in related investigations (Bouttier-Figueroa et al., 2023; Nistor & Butnariu, 2023). Overall, Phytochemicals having charged functional groups or donating electrons forming hydrogen bonds, or complexation and chelation, interact with oppositely charged nanoparticles through electrostatic forces, enhancing their stability. This stable interaction of plant extract chemicals - nanoparticles lowers the ability of the extract chemicals, including phytochemicals and sugars, to absorb UV light at certain characteristic structural regions like 356nm, which is strong evidence that confirms nanoparticle formation and their interaction with phytochemicals.

Table 4: The UV absorbance values for P and L at different concentration samples at 330 and 356nm

UV T×C	UV absorption at 330±4nm	UV absorption at 356±4nm
P (0.25%)	1.10	0.60
P (0.5%)	1.50	0.90
P (1%)	3.88	1.92
P (2%)	2.77	1.54
L (0.25%)	0.25	0.00
L (0.5%)	0.75	0.50
L (1%)	0.90	0.56
L (2%)	2.52	1.29

Regarding the extracts that include leaf with Zn and Ni nano particles; L × $ZnFe_2O_4$ (2%) showed the highest inhibition rate over 13 days (71% for the Zn-leaf interactions), the percent reduction in the UV absorbance compared to L (2%) was 64.3 and 58.8% at 330 and 356nm respectively (Table 3 and Table 4). For L × $NiFe_2O_4$ (1%) it showed a 56.0% inhibition rate over 13 days (for the Ni-leaf interactions) with a percentage reduction in the UV absorbance of 41.1 and 100.0% at 330 and 356nm, respectively, compared to L (1%). Regarding the pappus extracts with Zn and Ni nanoparticles; P × $ZnFe_2O_4$ (1%) showed the highest inhibition rate over 13 days (50% for the Zn-pappus interactions), the percent reduction in UV absorbance compared with P (1%) of 66.8% and 53.1% for 330 and 356nm, respectively. P × $NiFe_2O_4$ (0.25%) showed the highest inhibition rate (58.0%) for the Ni-pappus interactions over 13 days with a percent reduction in UV absorbance compared to P (0.25%) of 88.2% and 100.0%, respectively.

DISCUSSION

The results of this study showed a significant antifungal potential of green-synthesized $NiFe_2O_4$ and $ZnFe_2O_4$ nanoparticles (NPs) against *F. oxysporum* when used alone or in combination with *I. viscosa* plant extracts. The data confirmed that nanomaterials, particularly $NiFe_2O_4$, exhibit strong antifungal activity, with enhanced inhibition observed when combined with Percent Growth Rate (PGR).

The untreated *F. oxysporum* control exhibited the highest growth rates across all time points, underscoring its aggressive nature in the absence of antifungal interventions. $ZnFe_2O_4$ nanoparticles alone did not significantly curb fungal growth, indicating limited antifungal efficacy when used in isolation. Conversely, treatments incorporating $NiFe_2O_4$ nanoparticles, especially when combined with plant extracts (L × $NiFe_2O_4$ and P × $NiFe_2O_4$), demonstrated pronounced fungal growth suppression. Notably, the L × $NiFe_2O_4$ combination achieved the lowest growth rates (36.8% at 3 days, 31.1% at 8 days, and 34.1% at 13 days), suggesting a synergistic antifungal effect between the plant extracts and $NiFe_2O_4$ nanoparticles. Statistical analyses confirmed the significant impact of treatments and nanomaterials on fungal growth. Concentration factor did not markedly influence the inhibition trends, which suggested a non-significant effect. These observations align with previous studies that have reported the antifungal efficacy of $NiFe_2O_4$ nanoparticles against *F. oxysporum*. For instance, Sharma et al. (2022) synthesized $Ni_{0.5}Al_{0.5}Fe_2O_4$ nanoparticles and demonstrated their potent antifungal activity against *F. oxysporum*, achieving significant growth inhibition at specific concentrations. Similarly, studies have highlighted the potential of metal oxide nanoparticles as effective fungicides for plant disease control, emphasizing their role in inhibiting phytopathogenic fungi (Cruz-Luna et al., 2023).

At 3 days, treatments combining $NiFe_2O_4$ or $ZnFe_2O_4$ nanoparticles with plant extracts exhibited the highest inhibition rates, with L × $ZnFe_2O_4$ (61.4%) and L × $NiFe_2O_4$ (59.9%) being the most effective. In contrast, $ZnFe_2O_4$ alone (7.6%) and leaves extract alone (11.8%) showed minimal inhibition, indicating the limited antifungal activity of $ZnFe_2O_4$ when used alone. By 8 days, the combined treatments continued to show high inhibition rates (74.6% to 65.8%), while plant extracts alone and $ZnFe_2O_4$ alone remained less effective. At 13 days, the combined treatments maintained high inhibition rates (above 45%), confirming a sustained synergistic antifungal effect. However, the inhibition rates of nanoparticles alone and plant extracts alone decreased significantly over time. Statistical analyses revealed that

the effectiveness of treatments diminished over time, while the impact of nanomaterials remained significant, underscoring their crucial role in fungal inhibition. The significant interaction between treatments and nanomaterials further reinforces the enhanced antifungal activity observed when nanoparticles are combined with plant extracts.

Nanoparticles have a vast surface-to-volume ratio, which significantly enhances their property of cell membrane permeability. This can explain the case of interaction preparations, where the oxidized form of the active constituents is bonded to the surface of the nanoparticles and penetrates the cells in a better way (Bouttier-Figueroa et al., 2023). P × $NiFe_2O_4$ (0.5%) and L × $NiFe_2O_4$ (1%) showed percent inhibition rate over 13 days for the *F. oxysporum* of 29% and 56% respectively. This goes along with the previous reports about antimycotic activity of nickel nanoferrites on phytopathogenic fungi, where these compounds exhibited high ability to reduce and eradicate fungi. Nanomaterial fungicides: in vitro and in vivo antimycotic activity of cobalt and nickel Nano ferrites on phytopathogenic fungi (Sharma et al., 2017). In this study, the higher relative inhibition rate for the Ni-pappus and Ni-leaves preparations probably comes from the combined effect of Ni nanoferrites and in addition to the metal ligand interactions, in contrary for Zn ferrites alone were these compounds demonstrated almost very low to zero inhibition rates.

Nickel ferrite nanoparticles ($NiFe_2O_4$ and derivatives) are strong inhibitors of *F. oxysporum* by a two-pronged dual mechanism: direct cell-wall/membrane destruction and ROS–elicited oxidative stress. In vitro and pot-trial studies show that $NiFe_2O_4$ nanoparticles inhibit *F. oxysporum* infection very intensely—disease completely suppressed at ~500 ppm (0.5mg/mL) in pot culture conditions (Sharma et al., 2017; Sharma et al., 2022). The antifungal effect is generally attributed to ROS production—specifically singlet oxygen and hydroxyl radicals—resulting in lipid peroxidation, membrane destruction, and interference with fungal metabolism and survival (Chouhan et al., 2022). The inhibition of histidine (an ROS quencher) restored fungal growth after treatment with $Ni_{0.5}Al_{0.5}Fe_2O_4$ nanoparticles, demonstrating ROS as the primary cytotoxic effector (Sharma et al., 2022). Furthermore, the nanoparticles electrostatically interact with fungal cell surfaces, leading to membrane destabilization, leakage of intracellular contents, and inhibited spore germination, as documented in nickel–chitosan nanoconjugates against *F. oxysporum* (Chouhan et al., 2022; González-Merino et al., 2021; Ansari & Alomary, 2024). Thus, $NiFe_2O_4$ nanoparticles combine physical disruption and oxidative biochemical attack and hence are promising antifungal agents for agriculture. The synergistic antifungal effects observed in this study are consistent with previous research. For example, a study demonstrated that combining metal oxide nanoparticles with plant extracts significantly inhibited biofilm formation in pathogenic fungi, highlighting the potential of such combinations in enhancing antifungal efficacy (Bataineh et al., 2024). Additionally, the integration of nanoparticles with essential oils has shown promising synergistic antifungal efficacy, further supporting the potential of combining nanoparticles with natural products for enhanced antifungal activity (Sayed et al., 2024).

CONCLUSION

The integration of plant extracts of Clammy inula (*Inula viscosa* L) with Zn and Ni nanoferrites exhibits a synergistic antifungal effect against *F. oxysporum*, offering a promising strategy for managing this pathogen. Future research should focus on elucidating the mechanisms underlying this synergy and evaluating the practical applications of these findings in agricultural settings.

DECLARATIONS

Funding: The Authors would like to express gratitude to the Scientific Research and Innovation Support Fund, Ministry of Higher Education, for their financial support (project # AGR/1/22/2022), which covered the costs of essential materials required for the antagonistic analysis using the nanoparticles experiment, as well as other laboratory supplies.

Acknowledgement: The authors would like to thank the University of Jordan for facilitating this investigation.

Conflict of Interest: None.

Data Availability: All the data available in this article.

Author's Contribution: Conceptualization, W.M.O., K.M.A, and S.A; methodology, W.M.O, K.M.A, N.A.S, S.A AND A.A.; software, W.M.O and S.A; validation, W.M.O and S.A; investigation, W.M.O, N.A.S, K.M.A and S.A; resources, W.M.O, K.M.A and S.A; data curation, W.M.O AND S.A; writing original draft preparation, W.M.O, K.M.A and S.A; writing review and editing, W.O, K.M.A and S.A; funding acquisition, W.M.O and K.M.A.

Generative AI Statement: The authors declare that no Gen AI/DeepSeek was used in the writing/creation of this manuscript.

Publisher's Note: All claims stated in this article are exclusively those of the authors and do not necessarily represent those of their affiliated organizations or those of the publisher, the editors, and the reviewers. Any product that may be evaluated/assessed in this article or claimed by its manufacturer is not guaranteed or endorsed by the publisher/editors.

REFERENCES

Abou-Jawdah, Y., Wardan, R., Sobh, H., & Salameh, A. (2004). Antifungal activities of extracts from selected Lebanese wild plants against plant pathogenic fungi. *Phytopathologia Mediterranea*, 43(3), 377-386. https://doi.org/10.14601/Phytopathol_Mediterr-1761

Alghuthaymi, M.A., Rajkuberan, C., Rajiv, P., Kalia, A., Bhardwaj, K., Bhardwaj, P., Abd-Elsalam, K.A., Valis, M., & Kuca, K. (2021). Nanohybrid antifungals for control of plant diseases: Current status and future perspectives. *Journal of Fungi*, *7(1)*, 48.

https://doi.org/10.3390/jof7010048

Al-Hunaiti, A., Ghazzy, A., Sweidan, N., Mohaidat, Q., Bsoul, I., Mahmood, S., & Hussein, T. (2021). Nano-Magnetic NiFe2O4 and its photocatalytic oxidation of vanillyl alcohol—synthesis, characterization, and application in the valorization of lignin. *Nanomaterials*, 11(4), 1010. https://doi.org/10.3390/catal10080839

Al-Hunaiti, A., Mohaidat, Q., Bsoul, I., Mahmood, S., Taher, D., & Hussein, T. (2020). Synthesis and characterization of novel phyto-mediated catalyst, and its application for a selective oxidation of (VAL) into vanillin under visible light. *Catalysts*, 10(8), 839. https://doi.org/10.3390/catal10080839

Ansari, M.A., & Alomary, M.N. (2024). Bioinspired ferromagnetic $NiFe_2O_4$ nanoparticles: Eradication of fungal and drug-resistant bacterial pathogens and their established biofilm. *Microbial Pathogenesis*, *193*, 106729. https://doi.org/10.1016/j.micpath.2024.106729

Bataineh, S.M., Arafa, I.M., Abu-Zreg, S.M., Al-Gharaibeh, M.M., Hammouri, H.M., Tarazi, Y.H., & Darmani, H. (2024). Synergistic effect of magnetic iron oxide nanoparticles with medicinal plant extracts against resistant bacterial strains. *Magnetochemistry*, 10(7), 49. https://doi.org/10.3390/magnetochemistry10070049

Belabid, L., Simoussa, L., & Bayaa, B. (2010). Effect of some plant extracts on the population of *Fusarium oxysporum* f. sp. lentis, the causal organism of lentil wilt. *Advances in Environmental Biology*, 4(1), 95-101. https://www.aensiweb.com/old/aeb/2010/95-100.pdf

Boari, A., Vurro, M., Calabrese, G., Mahmoud, M., Cazzato, E., & Fracchiolla, M. (2021). Evaluation of *Dittrichia viscosa* (L.) Greuter Dried Biomass for Weed Management. *Plants*, 10(1), 147. https://doi.org/10.3390/plants10010147

Bouttier-Figueroa, D.C., Cortez-Valadez, M., Flores-Acosta, M., & Robles-Zepeda, R.E. (2023). Synthesis of metallic nanoparticles using plant's natural extracts: synthesis mechanisms and applications. *Biotecnia*, 25(3), 125-139. https://doi.org/10.18633/biotecnia.v25i3.1916

Chehri, K. (2011). Occurrence of Fusarium species associated with economically important agricultural crops in Iran. *African Journal of Microbiology Research,* 5(24), 4043-4048. https://doi.org/10.5897/ajmr10.158

Chouhan, D., Dutta, A., Kumar, A., Mandal, P., & Choudhuri, C. (2022). Application of nickel chitosan nanoconjugate as an antifungal agent for combating *Fusarium* rot of wheat. *Scientific Reports*, *12*(1), 14518. https://doi.org/10.1038/s41598-022-18670-2

Cruz-Luna, A.R., Vásquez-López, A., Rojas-Chávez, H., Valdés-Madrigal, M.A., Cruz-Martínez, H., & Medina, D.I. (2023). Engineered metal oxide nanoparticles as fungicides for plant disease control. *Plants*, 12(13), 2461. https://doi.org/10.3390/plants12132461

Edel-Hermann, V., & Lecomte, C. (2019). Current status of *Fusarium oxysporum* formae *speciales* and races. *Phytopathology*, 109(4), 512-530. https://doi.org/10.1094/PHYTO-08-18-0320-RVW

González-Merino, A.M., Hernández-Juárez, A., Betancourt-Galindo, R., Ochoa-Fuentes, Y.M., Valdez-Aguilar, L.A., & Limón-Corona, M.L. (2021). Antifungal activity of zinc oxide nanoparticles in *Fusarium oxysporum-Solanum lycopersicum* pathosystem under controlled conditions. *Journal of Phytopathology*, 169(9), 533-544. https://doi.org/10.1111/jph.13023

Grauso, L., Cesarano, G., Zotti, M., Ranesi, M., Sun, W., Bonanomi, G., & Lanzotti, V. (2020). Exploring Dittrichia viscosa (L.) Greuter phytochemical diversity to explain its antimicrobial, nematicidal and insecticidal activity. *Phytochemistry Reviews,* 19, 659-689. https://doi.org/10.1007/s11101-019-09607-1

Haoui, I. E., Derriche, R., Madani, L., & Oukali, Z. (2016). Extraction of Essential Oil from Inula viscosa (L.) Leaves: Composition, Antifungal Activity and Kinetic Data. *Journal of Essential Oil Bearing Plants*, 19(1), 108–118. https://doi.org/10.1080/0972060X.2015.1010598

Mamoci, E., Cavoski, I., Simeone, V., Mondelli, D., Al-Bitar, L., & Caboni, P. (2011). Chemical composition and *in vitro* activity of plant extracts from *Ferula communis* and *Dittrichia viscosa* against postharvest fungi. *Molecules*, 16(3), 2609-2625. https://doi.org/10.3390/molecules16032609

Nistor, A., & Butnariu, M. (2023). Physical Properties and Identification of Flavonoids by Ultraviolet-Visible Spectroscopy. *International Journal of Biochemistry & Physiology*, 8(2), 239. https://doi.org/10.23880/ijbp-16000239

Pane, C., Manganiello, G., Vitti, A., Celano, R., Piccinelli, A.L., & De Falco, E. (2023). Phytochemical Extracts of *Dittrichia viscosa* (L.) greuter from agroecological systems: Seed antigerminative properties and effectiveness in counteracting alternaria leaf spot disease on baby-leaf spinach. *Biology*, 12(6), 790. https://doi.org/10.3390/biology12060790

Qin, H., He, Y., Xu, P., Huang, D., Wang, Z., Wang, H., Wang, W., Zhao, Y., Tian, Q., & Wang, C. (2021). Spinel ferrites (MFe_2O_4): Synthesis, improvement and catalytic application in environment and energy field. *Advances in Colloid and Interface Science*, 294, 102486. https://doi.org/10.1016/j.cis.2021.102486

Rechek, H., Haouat, A., Hamaidia, K., Pinto, D.C., Boudiar, T., Válega, M.S., Pereira, D.M., Pereira, R.B., & Silva, A.M. (2023). *Inula viscosa* (L.) Aiton ethanolic extract inhibits the growth of human AGS and A549 cancer cell lines. *Chemistry & Biodiversity*, 20(3), e202200890. https://doi.org/10.1002/cbdv.202200890

Sayed, M.A., Ghazy, N.M., & El-Bassuony, A.A. (2024). Synergistic anti-dermatophytic potential of nanoparticles and essential oils combinations. *Journal of Inorganic and Organometallic Polymers and Materials*, 35, 1121-1135. https://doi.org/10.1007/s10904-024-03294-y

Shang, Y., Hasan, M.K., Ahammed, G.J., Li, M., Yin, H., & Zhou, J. (2019). Applications of nanotechnology in plant growth and crop protection: a review. *Molecules*, 24(14), 2558. https://doi.org/10.3390/molecules24142558

Sharma, P., Sharma, A., Sharma, M., Bhalla, N., Estrela, P., Jain, A., Thakur, P., & Thakur, A. (2017). Nanomaterial fungicides: in vitro and in vivo antimycotic activity of cobalt and nickel nanoferrites on phytopathogenic fungi. *Global Challenges*, 1(9), 1700041. https://doi.org/10.1002/gch2.201700041

Sharma, S., Kumari, P., Thakur, P., Brar, G.S., Bouqellah, N.A., & Hesham, A.E.-L. (2022). Synthesis and characterization of Ni0. 5Al0. 5Fe2O4 nanoparticles for potent antifungal activity against dry rot of ginger (*Fusarium oxysporum*). *Scientific Reports*, 12(1), 20092. https://doi.org/10.1038/s41598-022-22620-3

Shtacher, G., & Kashman, Y. (1970). 12-Carboxyeudesma-3, 11 (13)-diene. Novel sesquiterpenic acid with a narrow antifungal spectrum. *Journal of Medicinal Chemistry*, 13(6), 1221-1223. https://doi.org/10.1021/jm00300a047

Snyder, W.C., & Hansen, H. (1940). The species concept in Fusarium. *American Journal of Botany*, 27(2), 64-67. https://doi.org/10.1002/j.1537-2197.1940.tb14217.x

Vuko, E., Dunkić, V., Maravić, A., Ruščić, M., Nazlić, M., Radan, M., Ljubenkov, I., Soldo, B., & Fredotović, Ž. (2021). Not only a weed plant—biological activities of essential oil and hydrosol of *Dittrichia viscosa* (L.) greuter. *Plants*, 10(9), 1837. https://doi.org/10.3390/plants10091837

Zargar, M., Bayat, M., Saquee, F. S., Diakite, S., Ramzanovich, N. M., & Akhmadovich, K. A. (2023). New advances in nano-enabled weed management using poly (Epsilon-caprolactone)-based nanoherbicides: a review. *Agriculture,* 13(10), 2031. https://doi.org/10.3390/agriculture13102031

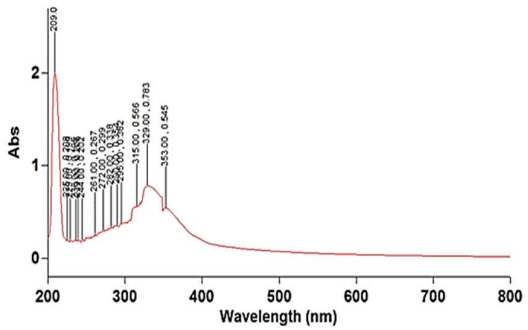

Fig. S1: UV-visible spectra of Leaves (1%).

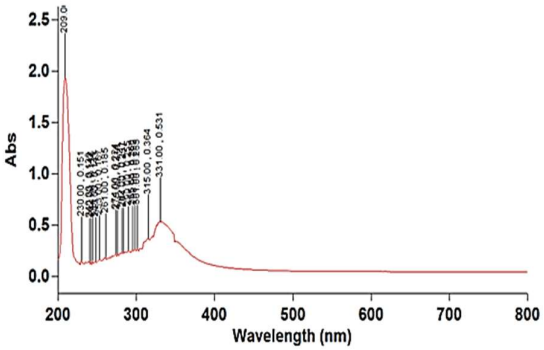

Fig. S2: UV-visible spectra of L×$NiFe_2O_4$ (1%).

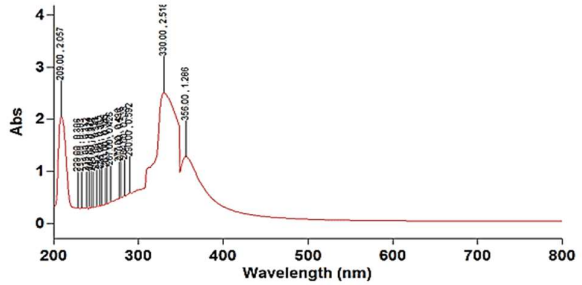

Fig. S3: UV-visible spectra of Leaves (2%).

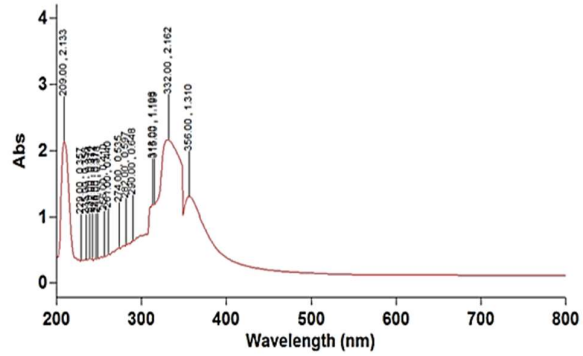

Fig. S4: UV-visible spectra of L×$ZnFe_2O_4$(2%).

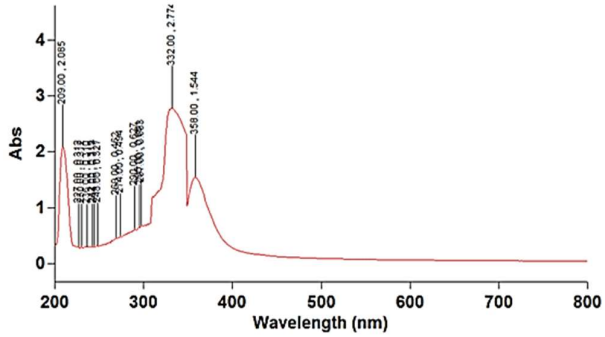

Fig. S5: UV-visible spectra of Pappus (1%).

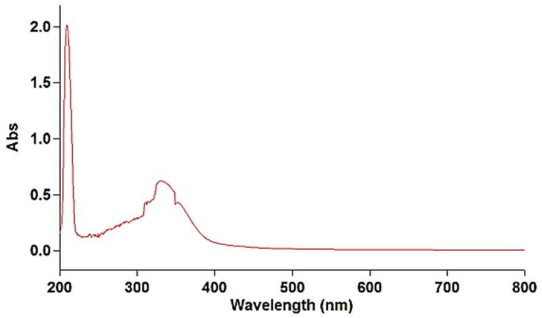

Fig. S6: UV-visible spectra of P×$NiFe_2O_4$ (1%).

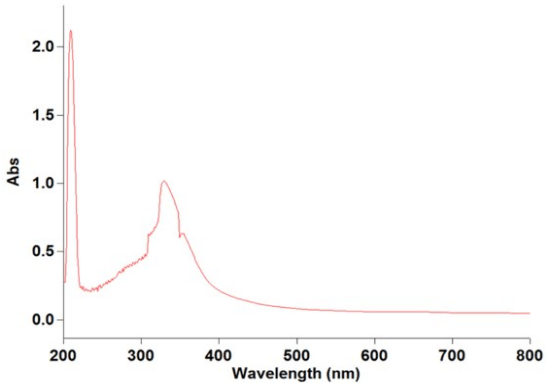

Fig. S7: UV-visible spectra of Pappus (0.25%).

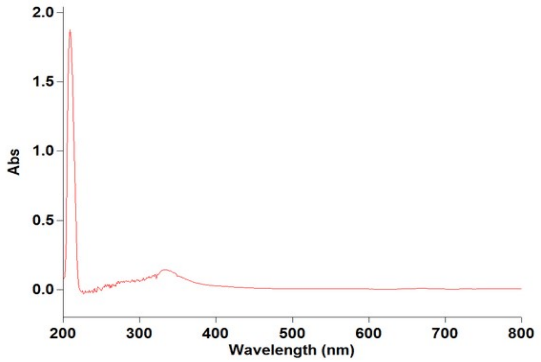

Fig. S8: UV-visible spectra of P×$NiFe_2O_4$ (0.25%).